

Measurement of small strains in thin epitaxial silicon films using photoelectron emission excited by an x-ray standing wave

M. V. Koval'chuk, V. G. Kon, and É. F. Lobanovich

A. V. Shubnikov Institute of Crystallography, Academy of Sciences of the USSR, Moscow

(Submitted June 9, 1985)

Fiz. Tverd. Tela (Leningrad) 27, 3379-3387 (November 1985)

Results are presented of experimental and theoretical studies of the angular dependence of the x-ray photoelectron yield from dynamic Bragg diffraction of x rays in silicon crystals with a homoepitaxial surface film. The study of the high-order (444) reflection gave a considerable increase in the sensitivity of the x-ray stationary wave method for photoelectron emission and an explicit determination, on the experimental curve, of the surface displacement due to lattice relaxation by small fractions of the interplanar spacing. Analytic expressions were obtained for the angular dependence of the photoemission in a bicrystal with any relationship between the parameters.

There have been many recent studies of the structure of damaged surface layers of semiconductor single crystals using the method of x-ray stationary waves for photoelectron emission. This method involves recording the angular dependence of the x-ray photoelectron yield from dynamic Bragg diffraction of x rays, when a stationary wave is formed in the crystal by the interference of coherent incident and reflected waves. When all photoelectrons leaving the crystal, with whatever energy, are recorded (integrated photoemission), the method yields information as to the structure of the surface layer averaged over a region whose thickness is of the order of the maximum photoelectron emergence depth L_{yi} . If $L_{yi} \ll L \ll L_{ex}$, where L is the thickness of the damaged layer and L_{ex} the extinction length, then it has been shown¹ that the method gives in principle the complete strain profile in the damaged layer, i.e., the depth variation of the interplanar spacing caused by the presence of defects, and the degree of disorder (amorphization) of the damaged layer. This information is contained in the tails of the angular distribution curves for the x-ray reflection and the photoemission, and a mathematical analysis of the experimental results is needed in order to obtain it.

The central part of the photoemission curve, which coincides with the angular range of total Bragg reflection, allows a direct determination of two quantities representing different features of the structural perfection of the surface layer with thickness L_{yi} . These are the coherent position $u(0)$ (the total displacement of the surface due to lattice relaxation in the damaged layer) and the coherent fraction $f = \exp[-W(0)]$, which gives the fraction of atoms that retain their regular positions in a reflecting plane.

This possibility was clearly demonstrated in a study (Refs. 2 and 3) of autoepitaxial films of germanium and of gallium arsenide, but hitherto it has not been possible to obtain corresponding results for silicon crystals. This is due primarily to the considerably greater degree of structural perfection of the homoepitaxial films of silicon that are actually used in semiconductor technology, and to their thinness.

Since in the central (phase-sensitive) part of the photoemission curve its profile is mainly governed by the phase factor¹ $\exp[ihu(0)]$, where h is a reciprocal lattice vector, it is clear that the sensitivity of the x-ray

standing wave method can be raised, in order to record small strains, by going to higher orders of reflections. In this case, we simultaneously solve the problem of increasing the extinction length in order to satisfy more fully the necessary condition $L_{yi} \ll L \ll L_{ex}$.

The present work is concerned with an experimental test of this idea. It shows clearly that the use of high orders of reflection allows a considerable increase in the sensitivity of the method. We were able to make the first experimental determination of the surface displacement in thin epitaxial films of silicon. Section 1 describes the experimental setup and results. In Sec. 2, we derive analytic expressions to calculate the angular dependence of the photoemission from a bicrystal. Section 3 gives a concluding discussion of the results.

1. EXPERIMENT

The measurements were done using a three-crystal x-ray spectrometer⁴ with an attachment for integral measurements of the photoemission. Silicon crystals were used with Cu $K\alpha$ radiation ($\lambda = 1.54 \text{ \AA}$) and a (444) dispersion-free two-crystal diffraction arrangement with asymmetric reflection in the monochromator; the angle between the incident beam and the crystal surface was 1° . To carry out the measurements, we first solved a methodological problem related to the photoemission measurement at high scattering angles. The reason is that unlike the earlier measurements on germanium and gallium arsenide crystals, made with the (440) reflection of Cu $K\alpha$ radiation, with Bragg angle $\theta_B = 47^\circ$, in the (444) case with silicon we have $\theta_B = 79^\circ$. The (111) orientation is one of the most widely used in microelectronics.

We solved this problem by constructing a special sample-holder which enabled us to fix the photoelectron detector (VEU-6) in the vacuum below the diffraction plane and immediately adjacent to the point of incidence of the x rays on the crystal. A BDS scintillation counter placed outside the vacuum recorded the reflected x-ray beam intensity from the crystal in vacuum. At the same time, a VEU-6 photomultiplier detected electrons entering the vacuum from the crystal.

The samples studied were silicon single crystals doped with antimony to a concentration of $3.7 \cdot 10^{19}$ atoms/cm³, on which was grown a homoepitaxial film of silicon doped with boron to a concentration of 10^{16} atoms/cm³.

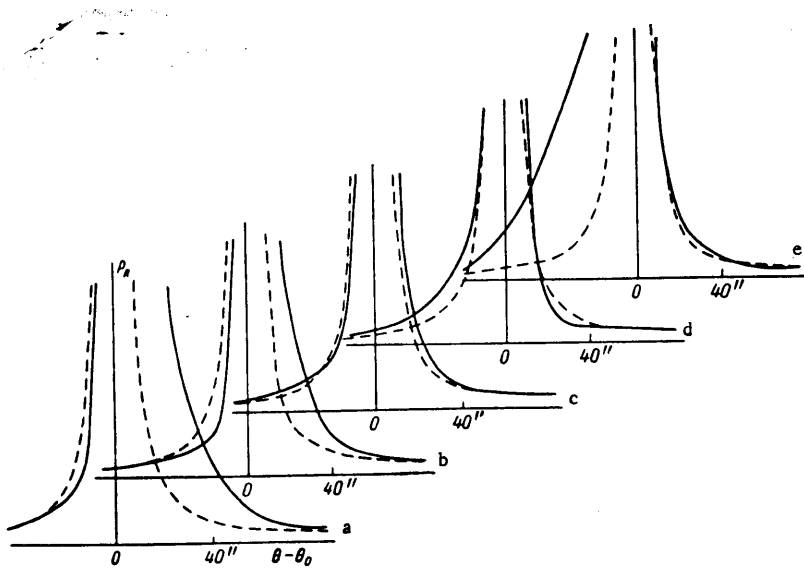


FIG. 1. X-ray diffraction reflection curves for silicon single crystals coated by a homoepitaxial film of silicon doped with boron and germanium, for various germanium concentrations.

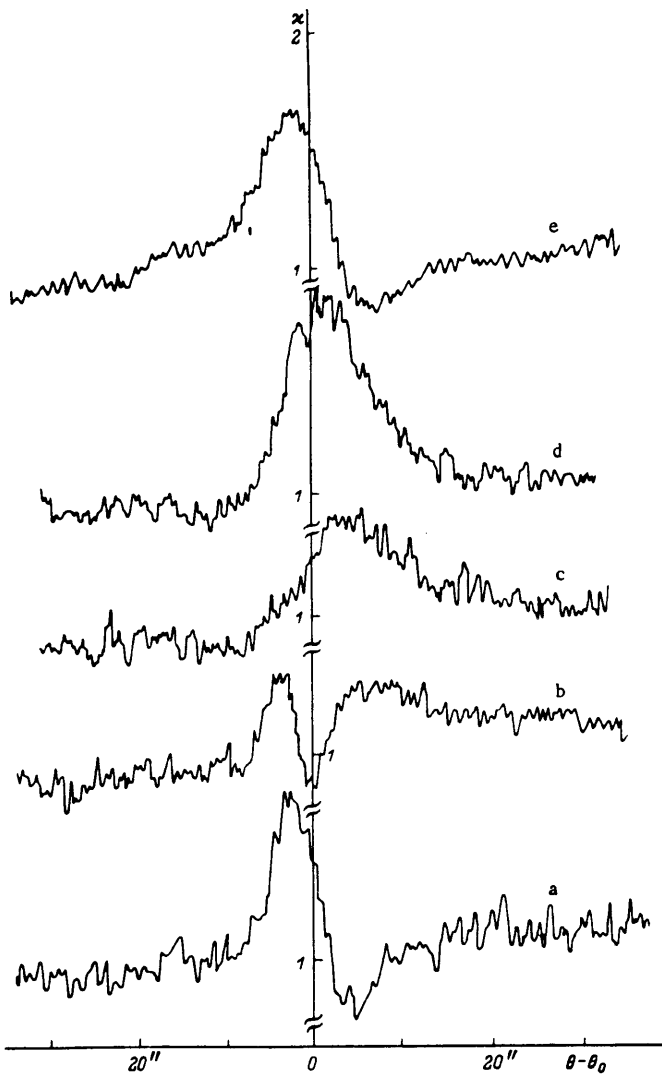


FIG. 2. Angular dependences of the photoemission for the same samples as in Fig. 1.

The film thickness was $L = 1.5 \mu$, whereas the extinction length $L_{ex} = 10.5 \mu$ in the case concerned, and $L_{y1} = 0.35 \mu$. All the films were grown under the same conditions (with the chloride process) on the same substrates,

except that germanium in concentrations between $3.7 \cdot 10^{19}$ and $1.5 \cdot 10^{20}$ atoms/cm³ was added uniformly, as well as the dopant to all except one film, which served as a control. The germanium doping was carried out during growth by reduction from the tetrachloride $GeCl_4$.

Figures 1 and 2 give the results of measurements for five films: the x-ray diffraction reflection curves (Fig. 1) and the angular dependences of the photoemission (Fig. 2). Let us first consider the diffraction reflection curves. In Fig. 1 (curve a), which corresponds to the original sample without germanium, there is a clear additional region of diffraction at the tail of the curve, for angles exceeding the Bragg angle ($\theta > \theta_B$). This means that the film is initially compressed relative to the substrate, i.e., the distance between the reflection (111) planes parallel to the surface is less in the film. The addition of germanium (with a larger covalent radius than that of silicon) to the film causes an expansion of the lattice, which increases with the germanium content. This follows immediately from the experimental results in curves b through e. As the germanium content increases, the rise of the curve in the range $\theta > \theta_B$ becomes less, and at $7 \cdot 10^{19}$ atoms/cm³ curve c is almost the same as the ideal curve, after which the strain changes sign. Curves d and e show a further diffraction region at angles $\theta < \theta_B$.

These strains are so small that the relative difference $\Delta d/d$ of the interplanar spacing in the film and in the substrate is of the order of 10^{-5} . With the relation $\Delta \theta = (\Delta d/d) \tan \theta_B$ for the change in the Bragg angle due to a lattice strain, we can easily see that with first-order reflection from the (111) plane ($\tan \theta_B = 0.254$) the additional diffraction region is within the substrate total reflection region. The width of the total reflection region decreases with increasing order of reflection. For this reason, our curves for first-order reflection from (111) planes have almost the ideal form.

Let us now look at the photoemission curves in Fig. 2. Whereas the central part of the diffraction reflection curves is almost the same for every sample, here we see a clear change in the form of the central (phase-sensitive) region. As already mentioned in the introduction, this change is due to the displacement of atomic planes in a

surface layer with thickness L_{y1} by an amount $u(0)$ relative to their positions in a perfect crystal, and to a partial amorphization of this layer [$e^{-W(0)} < 1$]. Although the displacement is very small, the use of a high-order reflection increases the phase $\varphi(0) = hu(0)$ to the values of the order of π in absolute magnitude. The minimum strain occurs in the sample corresponding to curve c. This photoemission curve is almost the same shape as the ideal curve. Curves a and e, on the other hand, are similar to each other, but have the opposite shape to curve c. We can therefore conclude at once that $\varphi(0) \approx -\pi$ for curve a and $\varphi(0) \approx \pi$ for curve e. For curves b and d, the phase has intermediate values. Thus, even a rapid glance at the photoemission curves is sufficient for a rough determination of the strain in the epitaxial film. More accurate information on the values of $u(0)$ and $W(0)$ can be obtained by means of a theoretical calculation, for instance by adjusting the theoretical curves to the experimental ones, using the least-squares method.

2. THEORY

A scheme has been developed⁶ for calculating the angular dependence of x-ray reflection and photoelectron emission in x-ray Bragg diffraction in crystals having a damaged surface layer. In general, when the lattice strain profile has any form, the chief problem is to solve the nonlinear differential equation for the ratio of the variable amplitudes $E_h(z)$ of the reflected wave and $E_0(z)$ of the incident wave (the reflection amplitude):

$$R(z) = \frac{E_h(z)}{E_0(z)} \left(\frac{\chi_h}{\chi_0} \frac{|\gamma_h|}{\gamma_0} \right)^{1/2} e^{i\varphi(z)}, \quad (1)$$

where $\varphi(z) = hu(z)$, χ_h and χ_h^- are the Fourier components of the crystal polarizability; γ_0 , γ_h are the cosines of the angles between the normal to the crystal surface and the wave vectors k_0 of the incident wave and $k_h = k_0 + h$ of the reflected wave ($\gamma_h < 0$), and z is the coordinate along the normal from the surface into the crystal. The equation is

$$\frac{dR}{dz} = \frac{2i}{L_{ex}} [y - iy_0 - Y(z)] R + \frac{i\tilde{C}}{L_{ex}} e^{-W(z)} (1 + R^2), \quad (2)$$

$$\left. \begin{aligned} y &= -\sqrt{\beta} \frac{\sin 2\theta_B}{|\chi_{rh}|} (\theta - \theta_0), \quad y_0 = \frac{\chi_{i0}}{|\chi_{rh}|} \frac{(1+\beta)}{2\sqrt{\beta}}, \quad \beta = \frac{\gamma_0}{|\gamma_h|}, \\ \tilde{C} &= C \frac{\sqrt{\chi_h \chi_h^-}}{|\chi_{rh}|}, \quad L_{ex} = \frac{\lambda \sqrt{\gamma_0 |\gamma_h|}}{\pi |\chi_{rh}|}, \\ Y(z) &= -\frac{1}{2} \frac{L_{ex}}{L_{ex}} \frac{d\varphi}{dz} = \pi \frac{L_{ex}}{d} \left(\frac{\Delta d(z)}{d} \right), \end{aligned} \right\} \quad (3)$$

$\exp[-W(z)]$ is the coherent fraction at depth z , C is the polarization factor, and θ_0 is the angle corresponding to the middle of the x-ray total reflection range.

Correspondingly, the direct wave amplitude is

$$E_0(z) = E_{i0} \exp \left\{ i \frac{\pi \chi_0}{\lambda \gamma_0} z - i \frac{\tilde{C}}{L_{ex}} \int_0^z dz' e^{-W(z')} R(z') \right\}. \quad (4)$$

The x-ray reflection coefficient at depth z is

$$P_R(z, y) = \left| \frac{\chi_h}{\chi_0} \right| |R(z, y)|^2 \quad (5)$$

(the observed value is for $z = 0$), and the photoelectron

yield is given by the dimensionless function

$$\kappa(y) = \frac{1}{N_\infty} \int_0^\infty dz P(z) I_0(z, y) \{1 + \beta P_R(z, y) + 2e^{-W(z)} \text{Re}[C_1 R(z, y)]\}, \quad (6)$$

$$\left. \begin{aligned} I_0 &= |E_0|^2, \quad N_\infty = \int_0^\infty dz P(z) I_0(z, \infty), \\ C_1 &= C \left(\frac{\chi_h}{\chi_0} \right)^{1/2} \frac{\chi_{i0}}{\chi_{i0}} \sqrt{\beta}. \end{aligned} \right\} \quad (7)$$

The function $P(z)$ is the probability that a photoelectron formed in the crystal at depth z reaches the detector.

For general functions $Y(z)$ and $W(z)$, Eq. (2) and the integrals in Eqs. (4) and (6) can be calculated only numerically. We shall derive some analytic expressions for $R(z, y)$ and $\kappa(y)$ in the particular case of a bicrystal consisting of a thick perfect substrate ($Y = W = 0$) and a layer with thickness L having constant $Y \neq 0$ and $W \geq 0$, that is, a layer that is partly subject to homogeneous amorphization and has an interplanar spacing that differs from that of the substrate.

In this case, the solution of Eq. (2) in $0 < z < L$ with the boundary condition $R(L) = R_0$, where

$$R_0(y) = -\frac{1}{C} [y - iy_0 + \sqrt{(y - iy_0)^2 - \tilde{C}^2}], \quad (8)$$

is

$$R(z, y) = \frac{x_1 - x_2 x_3 \exp(-\sigma(L-z))}{1 - x_3 \exp(-\sigma(L-z))}, \quad (9)$$

$$\left. \begin{aligned} x_1, x_2 &= -\frac{1}{C e^{-W}} [b \pm \sqrt{b^2 - C^2 e^{-2W}}], \quad b = y - iy_0 - Y, \\ x_3 &= \frac{x_1 - R_0}{x_2 - R_0}, \quad \sigma = \frac{1}{iL_{ex}} \sqrt{b^2 - C^2 e^{-2W}} = \sigma_r + i\sigma_i. \end{aligned} \right\} \quad (10)$$

In all these expressions, the square root is taken with a positive imaginary part. Equation (9) can be used to calculate the diffraction reflection curves for a crystal with a damaged surface layer containing several regions with constant Y and W , as has been done⁷ in the kinematic approximation.

Substituting the solution (9) in Eq. (4), we get an analytic expression for $E_0(z)$ and therefore for $I_0(z)$ in the range $0 < z < L$

$$I_0(z, y) = I_{i0} e^{-\mu_1(y)z} \left| \frac{1 - x_3 \exp(-\sigma(L-z))}{1 - x_3 \exp(-\sigma L)} \right|^2, \quad (11)$$

$$\mu_1(y) = \frac{\mu_0}{\gamma_0} - \frac{2y_0}{L_{ex}} + \sigma_r, \quad \mu_0 = \frac{2\pi}{\lambda} \chi_{i0}. \quad (12)$$

In the substrate ($L < z < \infty$),

$$I_0(z, y) = I_0(L, y) e^{-\mu_1(y)(z-L)}, \quad (13)$$

where the absorption coefficient $\mu(y)$ is $\mu_1(y)$ when $Y = W = 0$.

In order to carry out the integration in Eq. (6), it is necessary to know the explicit form of the influence function $P(z)$. The function most suitable for our case is that proposed by Liljequist,⁸ which has also been used elsewhere⁵:

$$P_L(z) = 1 - 2.01 \frac{z}{L_{yi}} + 1.02 \left(\frac{z}{L_{yi}} \right)^2, \quad z < L_{yi}. \quad (14)$$

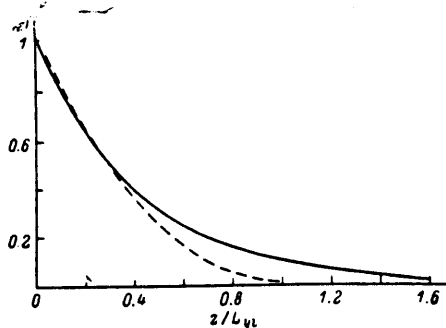


FIG. 3. Functions (14) (dashed curve) and (15) (continuous curve) for the probability of emergence of electrons on the surface.

However, in order to derive simple analytic expressions, without loss of accuracy, we shall use the exponential form

$$P(z) = \exp\left(-2.3 \frac{z}{L_{y1}}\right). \quad (15)$$

The coefficient here is chosen so that for small z the two functions are almost equal. The functions (14) and (15) are shown in Fig. 3. The influence function $P(z)$ is strictly exponential in the measurement of fluorescence radiation,⁹ and in that of the photo-emf in semiconductors having a p-n junction near the surface (a thin n-type layer).^{10,11}

On calculating the integral (6) with Eq. (15), we have finally

$$\kappa(y) = \frac{1}{N_{\infty}} I_0(L, y) e^{-\mu y L} (A_0(y) + A_L(y)), \quad (16)$$

$$A_0 = (\mu_{y1} + \mu)^{-1} [1 + C_2 |R_0|^2 + 2 \operatorname{Re}(C_1 R_0)], \quad (17)$$

$$A_L = |1 - x_3|^{-2} [\Phi_1 \Psi_1 + \Phi_2 \Psi_2 - \operatorname{Re}(\Phi_3 \Psi_3)], \quad (18)$$

$$\left. \begin{aligned} \Phi_k &= \frac{\exp(M_k L) - 1}{M_k}, \quad N_{\infty} = \left(\mu_{y1} + \frac{\mu_0}{\gamma_0}\right)^{-1} I_{0s}, \\ M_k &= \mu_{y1} + \frac{\mu_0}{\gamma_0} - \frac{2\mu_0}{L_{ex}} + \Delta_k, \quad \Delta_k = \begin{cases} \pm \sigma_r, & k=1, 2, \\ -i\sigma_i, & k=3; \end{cases} \end{aligned} \right\} \quad (19)$$

$$\left. \begin{aligned} \Psi_1 &= 1 + C_2 |x_1|^2 + \operatorname{Re}(C_3 x_1), \quad C_2 = \beta \left| \frac{\chi_h}{\chi_h} \right|, \\ \Psi_2 &= |x_2|^2 (1 + C_2 |x_2|^2 + \operatorname{Re}(C_3 x_2)), \quad C_3 = 2C_1 e^{-W}, \\ \Psi_3 &= x_3 [2(1 + C_2 x_2^* x_2) + C_3 x_2 + C_3^* x_1^*]. \end{aligned} \right\} \quad (20)$$

The parameter μ_{y1} signifies the reciprocal of the effective emergence depth for the secondary radiation. According to Eq. (15), in this case it is $\mu_{y1} = 2.3L_{y1}^{-1}$.

The expressions found are exact and are valid for any relationship between L , L_{ex} , and L_{y1} . They can also be used to analyze the angular dependence of the fluorescence or photo-emf yield. The convenience of the analytic expression in comparison with a direct numerical calculation lies in the possibility of explicitly separating the dependence on the various parameters. Also, the computing time for the fitting procedure is considerably shortened. Let us now take the simple case where $L_{y1} \ll L \ll L_{ex}$ and $|Y| \gg 1$. In the central part of the curve, $|y| < 1$, we then have $x_1 \approx 0$, $|x_2| \gg 1$, $x_3 \approx -R_0/x_2$, $\Psi_2 \approx C_2 |R_0|^2$, $\Psi_3 \approx -C_3 R_0$, $\sigma L = 1\varphi(0)$, $\varphi(0) = -2YL/L_{ex}$. Hence,

$$\kappa(y) \approx 1 + C_2 |R_0|^2 + 2 \operatorname{Re}(C_1 R_0 e^{\varphi(0)}) e^{-W}. \quad (21)$$

This result has already been discovered.¹ The calculation

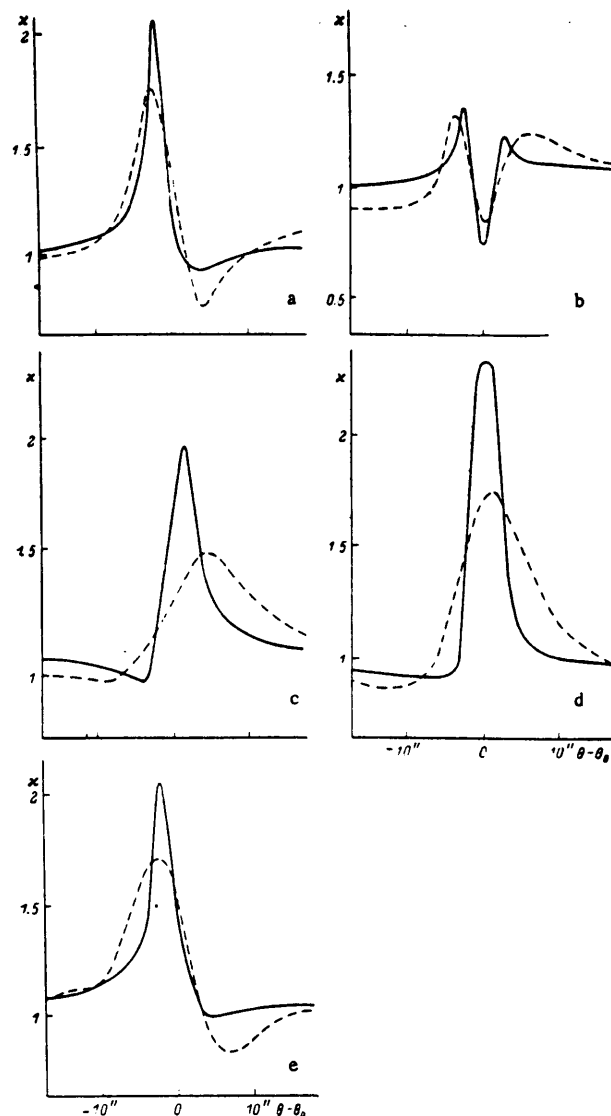


FIG. 4. Calculated (continuous curves) and experimental (dashed curves) angular dependences of photoemission excited by an x-ray standing wave.

from the more exact expressions (16)-(20) makes it easy to include minor effects of extinction and phase change at the photoelectron emergence depth.

3. DISCUSSION OF RESULTS

We calculated $\kappa(y)$ from Eqs. (16)-(20) for silicon, (444), $\text{CuK}\alpha$, $L_{y1} = 0.35 \mu$, $L = 1.5 \mu$, and for various values of Y and W , in order to obtain the best agreement between the theoretical and experimental curves. The observed points were normalized by using the least-squares method on selected points (31 at equal intervals over the whole angle range). The calculation took account of the convolution with the monochromator crystal reflection curve (asymmetry factor $\sqrt{\beta} = 0.22$). Figure 4 shows the calculated results and the experimental curves.

It is seen that the agreement achieved was not at all good. The experimental curves were considerably broader than the theoretical ones and somewhat irregular in shape. The discrepancy between the curves increases with the germanium content, i.e., from Fig. 4a to 4e. Despite the relatively low accuracy of the observations, this discrepancy is clearly outside the experimental error and

TABLE I. Values of the Parameters Y , W , $\varphi(0)/\pi$, and $\Delta d/d$

Sample	Y	W	$\varphi(0)/\pi$	$(\Delta d/d) \cdot 10^3$
a	-9.2	0.51	-0.84	-2.2
b	-6	0.25	-0.55	-1.4
c	-1	0.8	-0.09	-0.2
d	4	0.8	0.37	0.9
e	15	0.79	1.36	3.6

therefore has a physical cause. We have not, however, been able to elucidate the physical nature of the fact with sufficient certainty. The experimental diffraction reflection curves correlate well with those calculated; both the maximum value and the width of the total reflection region are practically the same. One possible cause of the discrepancy may be the presence of a block structure in the damaged layer, or surface roughness. To verify this, however, further measurements and calculations are needed.

Despite the lack of complete agreement between the theoretical and experimental curves, there is an obvious correlation between them. Table I shows the values of the parameters Y , W , φ , and $\Delta d/d$ corresponding to the theoretical curves. We may conclude that the present results give a clear demonstration of the availability of the x-ray standing wave technique for quantitative analysis of small strains in the surface layer of a crystal. Our procedure for obtaining the necessary relations between the positions of the wave field nodes and the atomic planes by adding germanium to the silicon lattice can be effective in compensating undesirable stresses in film-substrate type silicon structures. This can be done over a wide range of strain values, since germanium is an electrically inactive impurity and dissolves in silicon almost without limit.

The prospects for using this technique for the analysis of structural perfection are restricted by the need to measure the photoemission in high orders of reflection (which is not always possible with the vacuum method) and to satisfy the relations $L_{yi} \ll L \ll L_{ex}$. These difficulties can be effectively overcome by measuring the photoemission with a gas-flow proportional counter, as we first proposed.^{12,13} The design of the counter and its operating principles do not restrict the value of the Bragg angle. Moreover, it has been shown¹⁴⁻¹⁷ that a gas-flow proportional counter can be effectively used as an electron spectrometer with low resolution to change the elec-

tron emergence depth L_{yi} by selecting electrons with various energy losses. This property and the ability to choose any Bragg angle (order of reflection) enable us to vary L_{yi} and L_{ex} over wide ranges and ensure that $L_{yi} \ll L \ll L_{ex}$ for the damaged layers formed by a wide variety of methods.

- ¹A. M. Afanas'ev and V. G. Kon, Zh. Eksp. Teor. Fiz. **74**, 300 (1978) [Sov. Phys. JETP **47**, 154 (1978)].
- ²E. A. Sozontov, M. V. Kruglov, and B. G. Zakharov, Elektronnaya Tekh. Ser. 6, Mater. No. 7 (132), 108 (1979).
- ³E. A. Sozontov, M. V. Kruglov, and B. G. Zakharov, Phys. Status Solidi A **66**, 303 (1981).
- ⁴M. V. Koval'chuk, É. K. Kov'ev, and Z. G. Pinsker, Kristallografiya **20**, 142 (1975) [Sov. Phys. Crystallogr. **20**, 81 (1975)].
- ⁵A. I. Chumakov, G. V. Smitnov, M. V. Kruglov, and I. K. Solomin, Fiz. Tverd. Tela (Leningrad) **26**, 746 (1984) [Sov. Phys. Solid State **26**, 451 (1984)].
- ⁶V. G. Kohn and M. V. Kovalchuk, Phys. Status Solidi A **64**, 359 (1981).
- ⁷R. N. Kyutt, P. V. Petrashen, and L. M. Sorokin, Phys. Status Solidi A **60**, 381 (1980).
- ⁸D. Liljequist, Electron Penetration in Solids and its Application to Mössbauer Spectroscopy, USIP Report, Stockholm (1979).
- ⁹B. W. Batterman, Phys. Rev. **133**, A759 (1964).
- ¹⁰A. M. Afanas'ev, É. A. Manykin, É. F. Lobanovich, M. V. Koval'chuk, and R. M. Imamov, Fiz. Tverd. Tela (Leningrad) **24**, 2599 (1982) [Sov. Phys. Solid State **24**, 1473 (1982)].
- ¹¹S. I. Zheludeva, M. V. Koval'chuk, and V. G. Kon, Preprint IAÉ-3938/9 [in Russian], Institute of Atomic Energy, Moscow (1984).
- ¹²N. Hertel, M. V. Kovalchuk, A. M. Afanasev, and R. M. Imamov, Phys. Lett. A **75**, 501 (1980).
- ¹³M. V. Koval'chuk, S. S. Yakimov, R. M. Imamov, N. N. Faleev, Yu. N. Shilin, K. V. Serbinov, and V. Ya. Goncharov, Prib. Tekh. Eksp. No. 6, 185 (1981).
- ¹⁴M. V. Koval'chuk, R. M. Imamov et al., Abstracts of Papers presented at First All-Union Conf. on Methods and Apparatus for Studying the Coherent Interaction of Radiation and Matter, Simferopol', 1980 [in Russian], p. 55.
- ¹⁵M. V. Koval'chuk and É. Kh. Mukhamedzhanov, Fiz. Tverd. Tela (Leningrad) **25**, 3532 (1983) [Sov. Phys. Solid State **25**, 2033 (1983)].
- ¹⁶M. Bedzik, M. V. Koval'chuk, and G. Materlik, Metallofizika **6**, 101 (1984).
- ¹⁷M. V. Kovalchuk and E. Kh. Mukhamedzhanov, Phys. Status Solidi A **81**, 427 (1984).

Translated by J. B. Sykes